

Robustness Assessment of RC Frame Buildings under Column Loss Scenarios

Yihai Bao¹, Joseph A. Main², H.S. Lew³, and Fahim Sadek⁴

Engineering Laboratory, National Institute of Standards and Technology
100 Bureau Drive, Mail Stop 8611, Gaithersburg, MD 20899-8611

¹Tel: (301) 975-2061; E-mail: yihai.bao@nist.gov

²Tel: (301) 975-5286; E-mail: joseph.main@nist.gov

³Tel: (301) 975-6060; E-mail: hai.lew@nist.gov

⁴Tel: (301) 975-4420; E-mail: fahim.sadek@nist.gov

ABSTRACT

A computational assessment of the robustness of reinforced concrete (RC) building structures under column loss scenarios is presented. A reduced-order modeling approach is presented for three-dimensional RC framing systems, including the floor slab, and comparisons with high-fidelity finite element model results are presented to verify the approach. Pushdown analyses of prototype buildings under column loss scenarios are performed using reduced numerical models, and an energy-based procedure is employed to account for the dynamic effects associated with sudden column loss. The load-displacement curve obtained using the energy-based approach is found to be in good agreement with results from direct dynamic analysis of sudden column loss. A metric for structural robustness is defined by normalizing the ultimate capacity under sudden column loss by the applicable service-level gravity loading. The procedure is applied to two prototype 10-story RC buildings, one employing intermediate moment frames (IMFs) and the other employing special moment frames (SMFs). The SMF building, with its more stringent seismic design and detailing, is found to have greater robustness.

INTRODUCTION

Although a number of computational and experimental studies on the collapse resistance of reinforced concrete (RC) beam-column subassemblies or planar frames have been reported in recent years (e.g., Bao et al. 2008, Yi et al. 2008, Bao et al. 2012, Lew et al. 2011), limited studies have been done on three-dimensional RC frame systems including floor slabs. Previous studies of steel frame buildings have found that the floor slab contributes significantly to the collapse resistance of structures (e.g., Sadek et al. 2008, Main 2013). Experimental investigations on floor systems or realistic building structures can be very costly, limiting the number and scale of structural configurations that can be tested. Computational simulation provides an important complement to such testing by enabling the study of large, multi-story structures with various configurations. However, a challenge for

computational investigations is to develop reliable models that can be used in the analyses of large-scale structures without imposing prohibitive computational costs. In this study, experimentally validated models of planar frames (Bao et al. 2012) are extended to develop reduced models for three-dimensional frame systems including floor slabs. The reduced modeling approach is verified through comparison with high-fidelity finite element model results.

Using the reduced modeling approach, a robustness assessment procedure is proposed and illustrated using numerical examples. An energy-based approximate procedure for analysis of sudden column loss, previously proposed by Powell (2003) and Izzuddin et al. (2008), is also considered and verified computationally, which enables the structural capacity under sudden column loss to be evaluated using the results of a single pushdown analysis. A metric for structural robustness is defined by normalizing the ultimate capacity under sudden column loss by the applicable service-level gravity loading.

Two 10-story prototype buildings, which were designed for different seismic design categories, are evaluated for the potential loss of a first story column based on the proposed assessment approach. One building was designed for Seismic Design Category C (SDC C) and employs intermediate moment frames (IMFs), and the other was designed for Seismic Design Category D (SDC D) and employs special moment frames (SMFs). Full-scale beam-column assemblies from the prototype buildings have been tested to characterize the beam-to-column joint behavior (Lew et al. 2013) and to provide experimental data for validation of detailed and reduced numerical models (Bao et al. 2012). The results of the robustness assessment procedure show that the SMF building, with its more stringent seismic design and detailing, has greater robustness.

FLOOR SYSTEM MODELING

Two finite element models were developed to study the response characteristics of a two-bay by two-bay prototype floor system. One is a detailed model with a total of about 217,000 elements, including beam elements representing reinforcing bars and solid elements representing concrete. The other is a reduced model which consists of about 1700 shell elements representing the floor slab and 230 beam elements representing the beams and columns. A plan view of the prototype floor system is shown in Fig. 1 and reinforcement details are listed in Table 1. A bilinear stress-strain relationship is assumed for reinforcing bars with yield strength of 400 MPa and ultimate strength of 520 MPa. The corresponding plastic fracture strain is 15.6 %. The compressive strength of concrete is assumed to be 25 MPa.

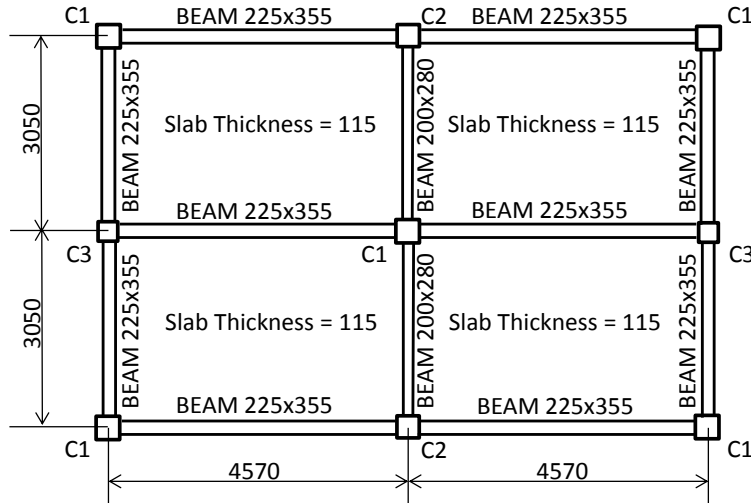
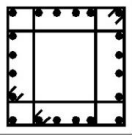
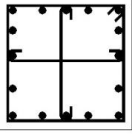
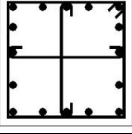


Fig. 1. Floor system plan view (units in mm).

Table 1. Reinforcement details (Units in mm).

BEAMS	Size (b × h)	Longitudinal reinforcement				Stirrups
		Ends		Mid		
		Top	Bottom	Top	Bottom	
Short span	225 × 355	four ø12	three ø12	three ø12	seven ø12 two layers	ø8 @ 150 (ends) ø8 @ 225 (mid)
Short span	200 × 280	three ø12	three ø10	three ø10	three ø12	ø8 @ 150 (ends) ø8 @ 225 (mid)
Long span	225 × 355	four ø12	three ø12	three ø12	seven ø12 two layers	ø8 @ 150 (ends) ø8 @ 150 (mid)
COLUMNS	Type	Size	Longitudinal reinforcement		Ties	
C1		350 × 350	twenty ø14		ø8 @ 125	
C2		330 × 330	sixteen ø14		ø8 @ 125	
C3		300 × 300	sixteen ø14		ø8 @ 125	
SLAB	two layers ø8 @ 200 top and bottom					

Note: Values following ø indicate bar diameter; values following @ indicate bar spacing (in mm).

Detailed modeling approach. An overview of the detailed model used in the analysis is shown in Fig. 2. The characteristic length of solid elements is between 20 mm and 35 mm. The length of beam elements ranges from 45 mm to 120 mm. Bond slip between beam longitudinal bars and surrounding concrete is modeled for interior beams only. A perfect bond is assumed for the other reinforcing bars, which are tied to the concrete using constraints. Concrete is modeled using a continuous surface cap model, which captures important features such as confinement effects and softening behavior both in compression and tension. By using a regulatory technique, it can achieve convergent softening behavior with reasonable mesh refinement. Reinforcing bars are modeled using an isotropic elastic-plastic model, in which effective stress versus plastic strain curves are defined separately for compression and tension. A plastic strain is also specified as the failure strain. Once the failure strain is reached, the corresponding element is removed from the analysis, simulating fracture of the reinforcing bar.

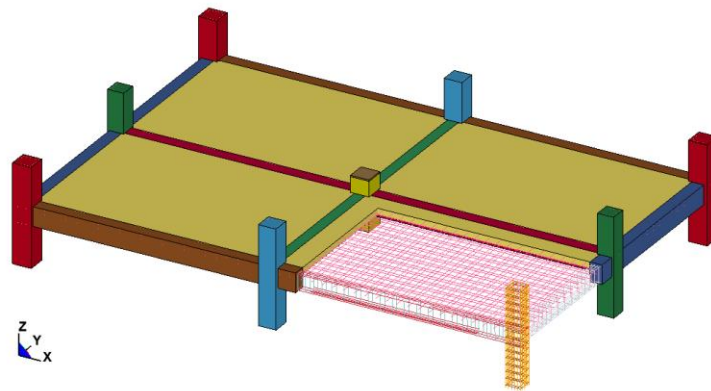


Fig. 2. Overview of detailed FE model

Reduced modeling approach. A reduced modeling approach for planar frames was developed previously by Bao et al. (2008), and this model was improved and validated by testing of two full-scale beam-column subassemblies (Bao et al. 2012). In this study, the reduced modeling approach is extended to include floor slabs in addition to beams, columns, and beam-column joints. Beams and columns are represented by one-dimensional elements with cross-section integration. Material properties are specified for each integration point of the discretized cross sections, with distinct material models for reinforcing bars, cover concrete and core concrete. Confinement effects are considered in the model for core concrete by specifying stress-strain curves corresponding to confined conditions. To avoid mesh dependency of the softening behavior, the ultimate strain is adjusted according to fracture energy and element size. Bond-slip effects are incorporated into the stress-strain relationship of reinforcing bars in interface zones near the beam-column joints, where extensive cracking can occur. More details on the modeling of beams and columns are provided by Bao et al. (2012).

The three-dimensional model of the beam-column joint region is developed by extending the planar model of Bao et al. (2012) and is illustrated in Fig. 3(a). The joint assembly comprises three rectangular frames composed of rigid links interconnected by hinges, with rotational springs representing the shear resistance in each of the three orthogonal planes. The joint shear behavior in orthogonal planes is assumed to be uncoupled. Line elements representing the beams and columns are connected to the joint assembly by defining multipoint constraints in which the rotational and translational degrees of freedom (DOFs) of nodes at the joint interface are interpolated from the translational DOFs of the four adjacent nodes in the joint assembly, as illustrated in Fig. 3(a).

The floor slab is modeled using layered shell elements with multiple integration points through the slab thickness. Material properties are specified for each integration point of the discretized slab, with distinct material models for reinforcing bars and concrete, as described previously for the beams and columns. Shell elements are connected to beam elements by nodal rigid body (NRB) constraints as depicted in Fig. 3(b). Nodes included in each NRB constraint are located in the same cross-sectional plane of the beam.

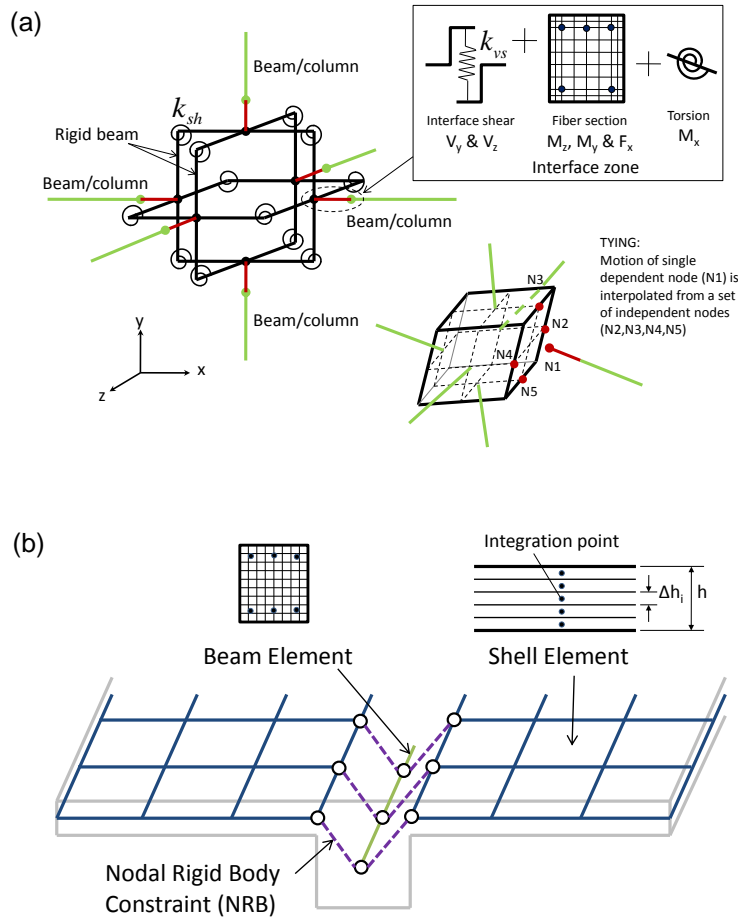


Fig. 3. (a) Three-dimensional joint model, and (b) floor system model.

Comparison of analysis results. Detailed and reduced models of the floor system in Fig. 1 are first compared without the floor slab. The exterior column bases were fixed and horizontal movement was restrained at the column tops. Vertical load was applied to the top of the interior column under displacement control until failure occurred. Fig. 4 shows computed curves of vertical load versus vertical displacement of the interior column, and good agreement is observed between the detailed and reduced models. The first load drop during the catenary action stage (at a vertical displacement of about 0.6 m) was due to the fracture of the beam-bottom reinforcing bars near the interior column at the short span beams. The ultimate load drop (at a vertical displacement of about 0.9 m) was caused by the fracture of the beam-top reinforcing bars at the same locations which eventually led to a system failure.

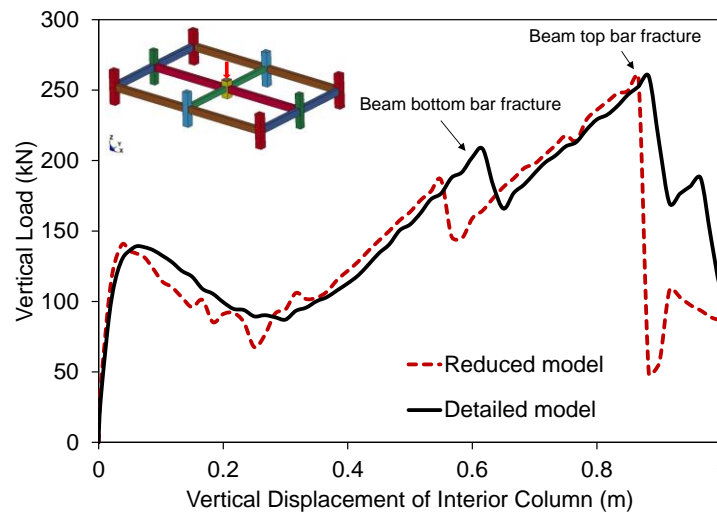


Fig. 4. Applied vertical load versus vertical displacement of interior column for 3D floor system without slab.

Detailed and reduced models are next compared with the floor slab included. To simulate a realistic loading condition under a column loss scenario, uniformly distributed loads were applied to the top of the slab and gradually increased until failure occurred. Load intensity was calculated by dividing the total vertical reaction at the column bases by the area of the floor slab, and curves of load intensity versus the vertical displacement from both detailed and reduced models are shown in Fig. 5, in which a close agreement is seen. The failure initiated at the top of the short span beams near the exterior columns where the beam longitudinal bars at the top and bottom fractured, followed by fracture of slab reinforcing bars in the same region. Both models showed a similar failure mode.

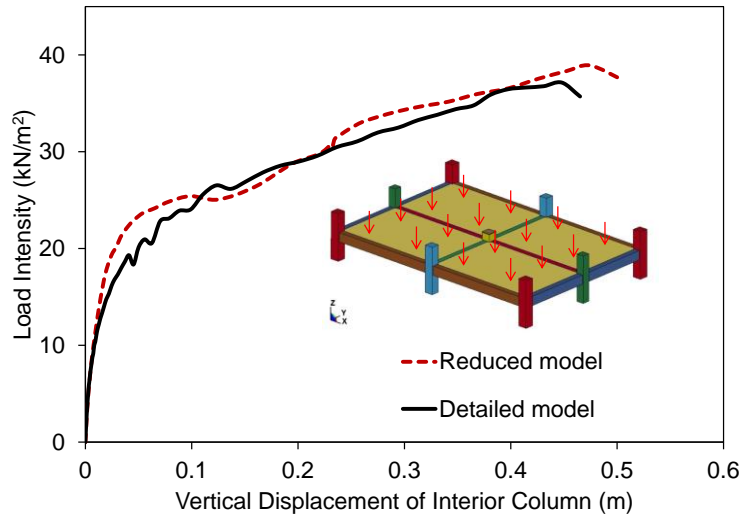
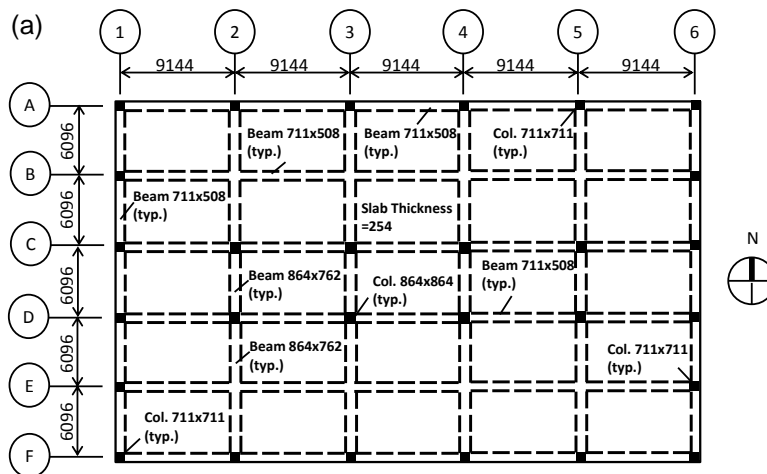


Fig. 5. Applied load intensity versus vertical displacement of interior column for 3D floor system with floor slab.

ASSESSMENT OF ROBUSTNESS

Two approaches for assessing structural robustness against sudden column loss are presented here. The first approach involves direct dynamic analysis of the structural response to sudden column loss. The second approach involves a static pushdown analysis, using an energy-based procedure to account for dynamic effects associated with sudden column loss. Two prototype buildings, which were designed for Seismic Categories C and D, and which incorporate intermediate moment frames (IMFs) and special moment frames (SMFs), respectively, are evaluated using these approaches. Fig. 6 shows the plan layouts of the prototype IMF and SMF buildings, and further information on the prototype building designs is provided by Lew et al. (2011).



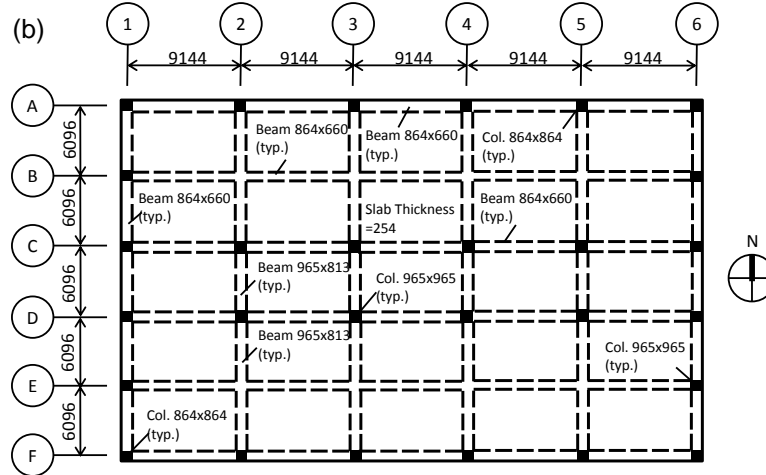


Fig. 6. Plan layout of prototype buildings: (a) IMF building; (b) SMF building (units in mm).

The service-level gravity load intensity adopted in these analyses, denoted G , is based on the load combination specified in ASCE 7-10 (ASCE 2010, Section 2.5.2.2) for assessing the residual capacity of structural systems following the notional removal of load-bearing elements:

$$G = 1.2D + 0.5L \quad (1)$$

where D is dead load and L is live load. Table 2 summarizes the gravity loading applicable to the two prototype buildings considered in this study. The gravity loading for the SMF building is somewhat larger than for the IMF building because of the larger self-weight associated with the larger beam dimensions (see Fig. 5).

In analyzing structural responses to column loss, as described in the following sections, the service-level gravity loading G is applied to the floor slab in bays unaffected by the column removal, while a higher-intensity loading is applied to the bays adjoining the removed column, in order to assess the ultimate load intensity that can be redistributed by the structural system. The ultimate capacity under sudden column loss is normalized by the service-level gravity loading G to define a metric for structural robustness.

Table 2. Gravity loads for prototype buildings.

Gravity Load Type	IMF Building		SMF Building	
	Floors	Roof	Floors	Roof
Self-weight (kN/m^2)	7.18	7.18	8.14	8.14
Superimposed dead load (kN/m^2)	1.44	0.48	1.44	0.48
Total dead load, D (kN/m^2)	8.62	7.66	9.58	8.62
Live load, L (kN/m^2)	4.79	1.20	4.79	1.20
Combined gravity load, G (kN/m^2)	12.74	9.79	13.89	10.94

Direct dynamic analysis. To illustrate the direct dynamic analysis procedure, a single floor from the prototype IMF building is considered, with columns extending one story above and below. As shown in Fig. 7, the service-level gravity loading G is applied to the floor slab in bays unaffected by the column removal, while a higher load intensity of $\lambda_d G$ is applied to the bays adjoining the column to be removed (column D5 in Fig. 7). The dimensionless factor λ_d represents the normalized load intensity applied to the affected bays, with $\lambda_d > 1$ indicating loads in excess of the service-level gravity loading. The subscript d in the factor λ_d denotes *dynamic*, indicating that the analysis considers the dynamic response to sudden column removal under the specified gravity loading.

Before column removal, the gravity load is gradually applied to the floor system over a period of 3 s and is held constant for an additional 0.5 s to avoid introduction of spurious dynamic effects. After the gravity initialization (at $t = 3.5$ s), the column is removed instantaneously. The time-varying vertical displacement of column D5 under a normalized load intensity of $\lambda_d = 2$ is plotted in Fig. 7, showing that the structural system is able to redistribute the applied gravity loading with a peak dynamic displacement of $\Delta_p = 560$ mm. A load versus displacement curve for sudden column loss can be generated by repeating this analysis procedure for different values of the normalized load intensity ($\lambda_{d1}, \lambda_{d2}, \lambda_{d3}, \dots$) and calculating the corresponding peak dynamic displacements ($\Delta_{p1}, \Delta_{p2}, \Delta_{p3}, \dots$), as illustrated in Fig. 8 for column D5. The maximum value of the normalized load intensity that can be sustained without collapse is denoted $\lambda_{d,u}$, and this quantity is proposed as a metric of structural robustness. Values of $\lambda_{d,u} < 1$ indicate that a structure cannot sustain the service-level gravity loading under sudden column loss, while larger values of $\lambda_{d,u}$ indicate greater resistance to collapse. The analysis results in Fig. 8 show a normalized ultimate capacity of $\lambda_{d,u} = 2.75$, indicating that the structure can sustain 2.75 times the service-level gravity loading under sudden column loss, with a corresponding peak dynamic displacement of $\Delta_p = 1600$ mm.

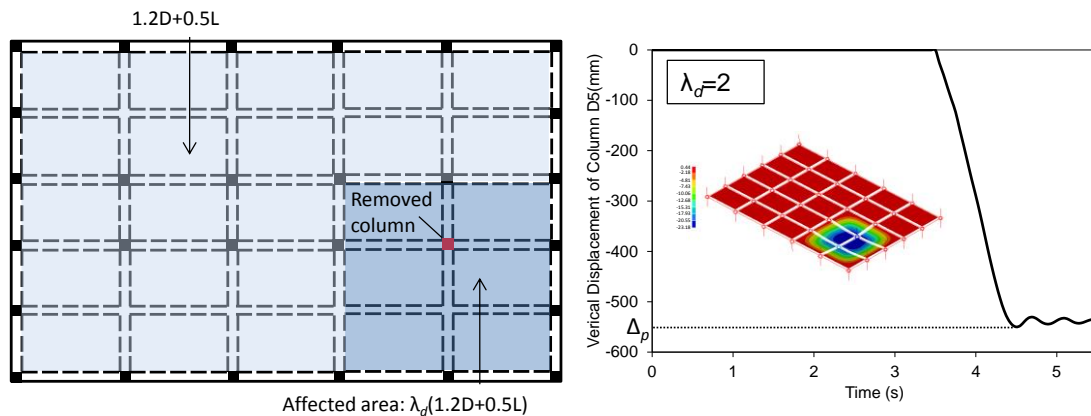


Fig. 7. Direct dynamic analysis of IMF floor system.

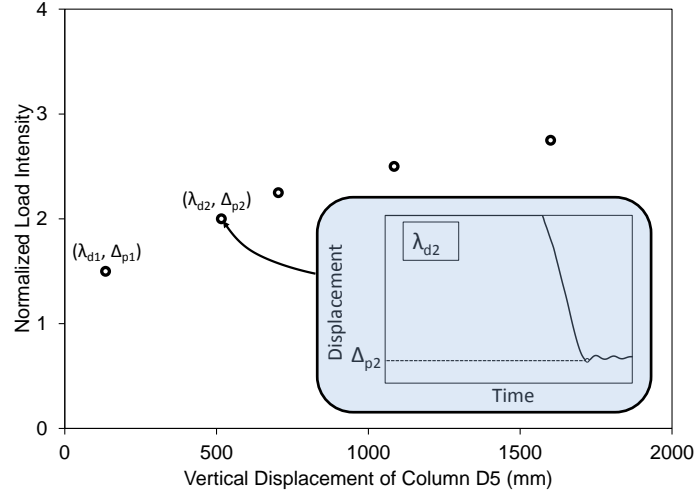


Fig. 8. Direct dynamic analysis procedure for generating load versus displacement curve for sudden column loss.

Approximate analysis based on energy balance. The direct dynamic analysis procedure requires a series of dynamic analyses to be performed at different load intensities in order to determine the ultimate capacity of the structural system under sudden column loss. However, by considering energy balance, the dynamic effects associated with sudden column loss can be accounted for without doing a dynamic analysis (Powell 2003, Izzuddin et al. 2008, Main 2013). Using this approach, a load versus displacement curve for sudden column loss can be generated more efficiently from the results of a single static pushdown analysis. In the static pushdown analysis, the missing column is removed prior to loading, and gravity loading is applied in the same pattern as illustrated in Fig. 7, with service-level gravity loading G in unaffected bays and loading of $\lambda_s G$ applied to bays adjoining the missing column. In the pushdown analysis, the factor λ_s is increased from zero until the ultimate capacity is reached, and a curve of normalized load intensity versus vertical column displacement is thus obtained, denoted $\lambda_s(\Delta)$, where the subscript s denotes *static*.

The energy-based procedure is based on the assumption that the structure responds in a single mode of deformation under static or dynamic loading. At the instant of peak dynamic displacement after sudden column loss, the kinetic energy must be zero; therefore, the loss of external potential energy W_{ext} equals the gain in internal energy W_{int} :

$$W_{ext} = \alpha \lambda_d G \Delta_p \quad (2)$$

$$W_{int} = \alpha \int_0^{\Delta_p} \lambda_s(\Delta) G d\Delta \quad (3)$$

$$W_{ext} = W_{int} \Rightarrow \lambda_d \Delta_p = \int_0^{\Delta_p} \lambda_s(\Delta) d\Delta \Rightarrow \lambda_d = \frac{1}{\Delta_p} \int_0^{\Delta_p} \lambda_s(\Delta) d\Delta \quad (4)$$

where α is a constant related to deformation mode, G is the service-level gravity load, and Δ_p is peak dynamic displacement. Eq. (4) indicates the hatched area equals the shaded area as shown in Fig. 9. By applying Eq. (4) for different values of Δ_p , a curve $\lambda_d(\Delta)$ can be obtained, shown as dashed in Fig. 9, which relates the normalized load intensity to the peak dynamic displacement under sudden column loss.

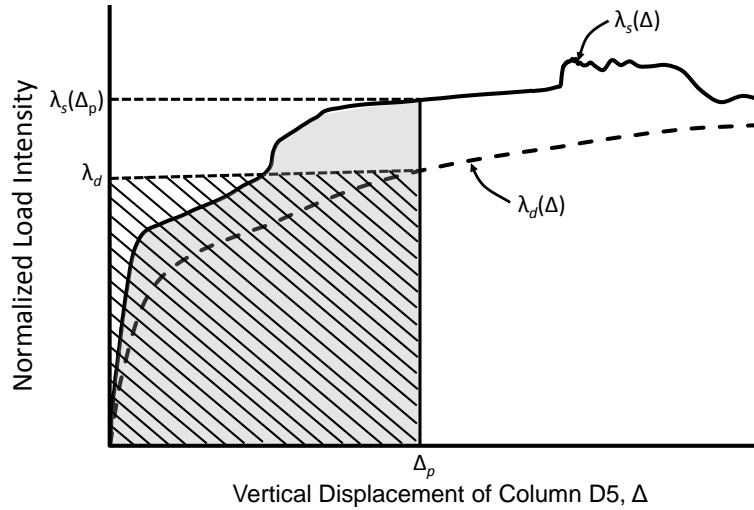


Fig. 9. Approximate procedure for generating load versus displacement curve for sudden column loss.

The above approach is verified by comparing direct dynamic analysis results with results of the energy-based approximate analysis for a single floor from the prototype IMF building under the loss of column D5 (see Fig. 7). In Fig. 9 the solid curve, denoted $\lambda_s(\Delta)$, was obtained from the pushdown analysis, while the dashed curve, denoted $\lambda_d(\Delta)$, was obtained from the energy-based analysis using Eq. (4). The open circles represent results from direct dynamic analysis of sudden column loss under various load intensities, previously plotted in Fig. 8. Good agreement is observed between the dashed line and the open circles in Fig. 10, verifying the accuracy of the energy-based approximate analysis of sudden column loss.

Ultimate capacity under sudden column loss. The displacement corresponding to the ultimate static load intensity is used as the limit state in assessing structural capacity under sudden column loss in this study. Fig. 10 shows that $\lambda_d(\Delta)$ continues to increase somewhat for displacements exceeding Δ_u . However, uncertainties in model predictions increase significantly in the post-ultimate response, and the assumption of an unchanging mode of deformation may also become less appropriate after the ultimate load has been exceeded and a collapse mechanism has been formed. For these reasons, and for the sake of conservatism, the ultimate capacity under column loss, denoted $\lambda_{d,u}$, is evaluated at the displacement Δ_u corresponding to the ultimate static load, as illustrated in Fig. 10. Using this approach, a value of $\lambda_{d,u} = 2.66$ is obtained (plotted with a solid circle), which is 3.3 % less than the value of $\lambda_{d,u} = 2.75$

obtained previously from direct dynamic analysis (the right-most open circle in Fig. 10). This confirms that the proposed ultimate capacity estimate using energy-based analysis is slightly conservative.

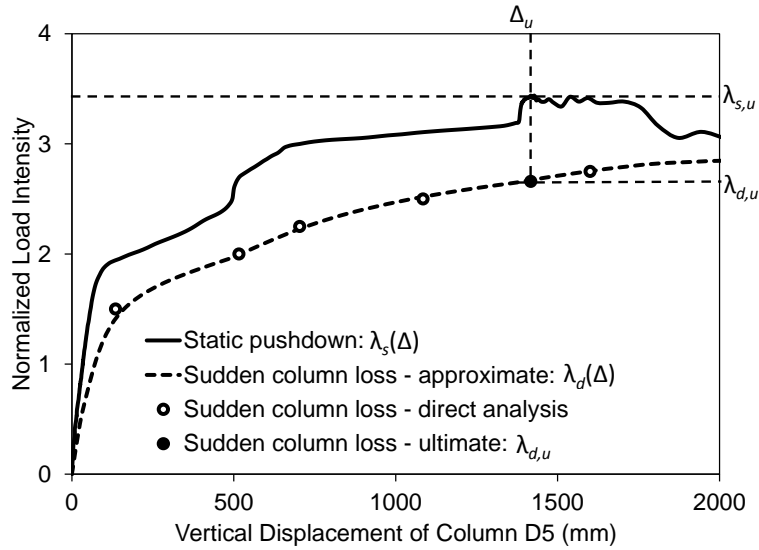


Fig. 10. Comparison of load versus displacement responses from direct and approximate analyses of sudden column loss of IMF floor system.

Analysis of prototype buildings. The robustness assessment procedures are now applied to the two 10-story prototype buildings to assess robustness against sudden loss of column D5 at the first-story level, and results are shown in Fig. 11. Fairly good agreement is observed between the results of direct dynamic analysis (open circles) and energy-based analysis (dashed curve), although discrepancies for the 10-story buildings are larger than previously observed for a single floor (Fig. 10). For both buildings, the ultimate static capacity under pushdown loading was associated with failure of column F5, with failure occurring in the first story for the IMF building and in the second story for the SMF building. Normalized ultimate capacities of $\lambda_{d,u} = 1.29$ and $\lambda_{d,u} = 2.08$ are obtained for the IMF and SMF buildings respectively, which are plotted with solid circles in Fig. 11 at displacements of Δ_u . Using $\lambda_{d,u}$ as the robustness metric, it can be concluded that the SMF building has greater robustness than the IMF building under sudden loss of column D5 at the first-story level. To assess the overall robustness of a structure, all applicable column removal scenarios should be considered, and the overall robustness index for the structure would be the minimum value of $\lambda_{d,u}$ obtained from all cases.

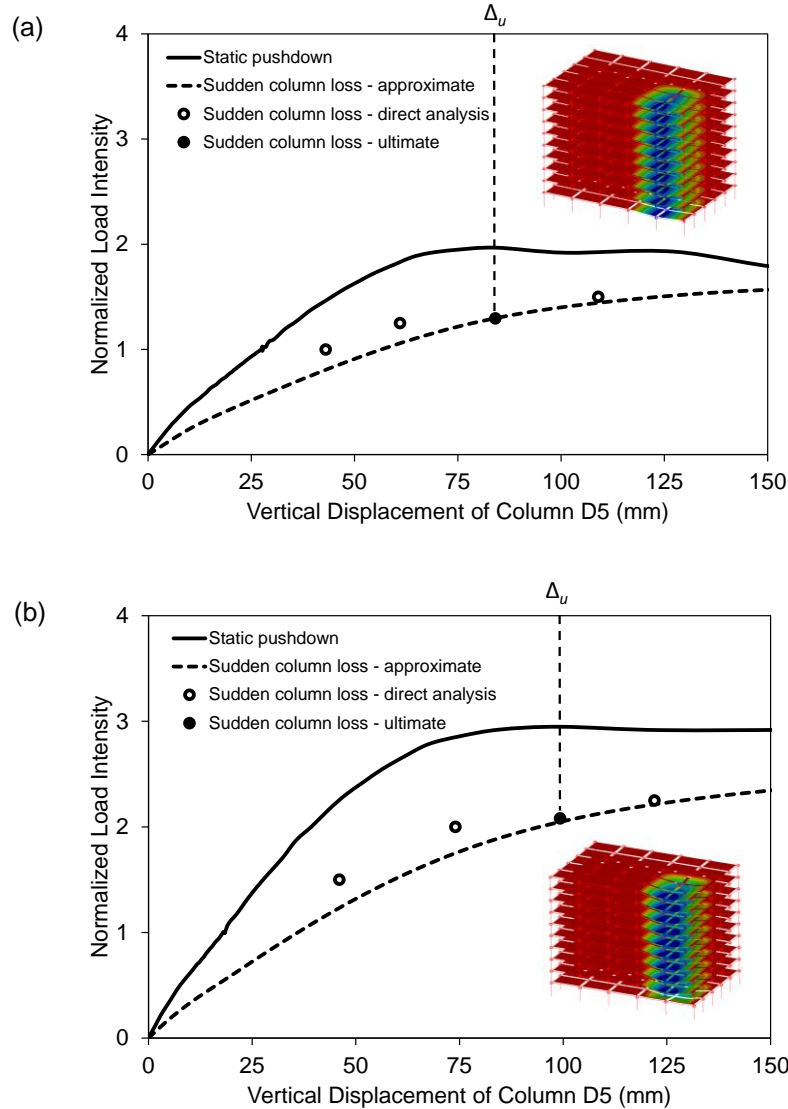


Fig. 11. Robustness assessment of (a) IMF building and (b) SMF building under sudden loss of first story column D5.

CONCLUSIONS

A reduced modeling approach for three-dimensional RC frame systems with floor slabs was presented, and good agreement between detailed and reduced model results was observed, providing verification that the reduced models can capture the essential structural responses and failure modes. An energy-based approximate procedure for analysis of sudden column loss was described that uses the results of a nonlinear static pushdown analysis, and this procedure was also verified through comparison with results of direct dynamic analysis. A procedure for robustness assessment was proposed, and a metric for structural robustness was defined by normalizing the ultimate capacity under sudden column loss by the applicable service-level gravity loading. This procedure was used to evaluate two prototype 10-story buildings under

a first-story column loss scenario, and the results showed that the SMF building, with its more stringent seismic design and detailing, had greater robustness than the IMF building.

ACKNOWLEDGMENT

Sam-Young Noh of Hanyang University is gratefully acknowledged for his valuable input in the development of the robustness assessment procedure during his one-year tenure as a Guest Researcher at NIST.

REFERENCES

- American Society of Civil Engineers (ASCE). (2010). "Minimum design loads for buildings and other structures." *ASCE/SEI 7-10*, Reston, VA.
- Bao, Y., Kunnath, S. K., El-Tawil, S., and Lew, H. S. (2008). "Macromodel-based simulation of progressive collapse: RC Frame Structures." *J. Struct. Eng.*, 134(7), 1079-109.
- Bao, Y., Lew, H.S., and Kunnath, S. (2012). "Modeling of reinforced concrete assemblies under a column removal scenario," *J. Struct. Eng.*, In press, available online (DOI:10.1061/(ASCE) ST.1943-541X.0000773).
- Izzuddin, B.A., Vlassis, A.G., Elghazouli, A.Y., and Nethercot, D.A. (2008). "Progressive collapse of multistory buildings due to sudden column loss – Part I: Simplified assessment framework." *Eng. Struct.*, 30, 1308-1318.
- Lew, H.S., Bao, Y., Sadek, F. Main, A. J., Pujol, S., and Sozen, M. A. (2011). "An experimental and computational study of reinforced concrete assemblies under a column removal scenario," *NIST TN 1720*, National Institute of Standards and Technology, Gaithersburg, MD.
- Lew, H.S., Bao, Y., Pujol, S., and Sozen, M.A. (2013). "Experimental study of RC assemblies under a column removal scenario." *ACI Structural Journal*, in press.
- Main, J.A. (2013). "Composite floor systems under column loss: collapse resistance and tie force requirements." *J. Struct. Eng.*, in press.
- Main, J.A., and Sadek, F. (2012). "Robustness of steel gravity frame systems with single-plate shear connections," *NIST TN 1749*, National Institute of Standards and Technology, Gaithersburg, MD.
- Powell, G. (2003). "Collapse analysis made easy (more or less)." *Proc. Annual Meeting of the Los Angeles Tall Buildings Structural Design Council*, Progressive collapse and blast resistant design of buildings.
- Sadek, F., El-Tawil, S., and Lew, H.S. (2008). "Robustness of composite floor systems with shear tab connections: modeling, simulation, and evaluation." *J. Struct. Eng.*, 134(11), 1717-1725.
- Yi, W., He, Q., Xiao, Y., and Kunnath, S.K. (2008). "Experimental study on progressive collapse-resistant behavior of reinforced concrete frame structures." *ACI Struct. J.*, 105(4), 433-439.